Bistability of flame propagation in a model with competing exothermic reactions

I. N. Towers[a], V. V. Gubernov[b], A. V. Kolobov[b], A. A. Polezhaev[b], H. S. Sidhu[a]

[a] *School of Physical, Environmental and Mathematical Sciences, University of New South Wales at the Australian Defence Force Academy, Northcott Drive, Canberra ACT 2600 Australia*

[b] *I. E. Tamm Theory Department, P. N. Lebedev Physical Institute of the Russian Academy of Sciences, 53 Leninsky prospect, Moscow, 119991 Russia*

Abstract

In this paper we investigate a diffusional-thermal model with two-step competitive exothermic reactions for premixed combustion wave propagation in one spatial dimension under adiabatic conditions. A criterion based on the crossover temperature notion was used to qualitatively predict the region in the space of parameters where three travelling combustion wave solutions co-exist, which are further studied via numerical means. It is demonstrated that under certain conditions the flame speed is an 'S'-shaped function of parameters. The fast branch is either stable or is partly stable and exhibits the Andronov-Hopf bifurcation before the turning point is reached. The mid branch is completely unstable. The slow solution branch is either unstable or partly stable and exhibits a single or a pair of Andronov-Hopf bifurcations. The Andronov-Hopf bifurcations are shown to be supercritical giving rise to stable pulsating waves. Bistability and hysteresis phenomena are also demonstrated.

Keywords: combustion waves, competitive reactions, bistability, oscillatory instabilities

Email address: i.towers@adfa.edu.au (I. N. Towers)

1. Introduction

Combustion waves with two-stage competing exothermic reactions $A \to B$ and $A \to C$ have been studied experimentally [1, 2], analytically [3–7] and numerically [5]. In [1, 2] the experimental observation of bistability of flame propagation is reported for combustion of Me-C-H_2, where Me is either Ti or Zr. Here and later on by term bistability the co-existence of two stable travelling combustion waves is meant. In this system the reaction can proceed along two competing paths with different end products, either metal carbo-hydrides or metal hydrides. The first reaction channel is characterized by high combustion velocity and temperature, while the latter by low combustion wave speed and burning temperature. Depending on the experimental parameters: hydrogen pressure, mixture composition etc., there exist conditions that both regimes of flame propagation can be realized by using high or low temperature ignition sources. It is also demonstrated that changing the control parameters may also lead to the disappearance of the bistable regime of flame propagation.

The first analytical investigation of combustion waves with two-stage exothermic reactions dates back to 1975 [3]. In this paper by Berman and Riazantsev the diffusional-thermal model for the planar flame propagation is studied by using the activation energy asymptotic (AEA) method. The flame temperature and speed are calculated for cases of gaseous and solid fuel. Although it is not explicitly formulated in this paper and it is not directly acknowledged in the latter publications [4, 5, 8], the analytical results of [3] suggest that the dependence of the flame speed and burning temperature on parameters can be multi-valued 'S'-shaped function of parameters. There are either three solutions travelling with different velocities or a single solution depending on the parameters of the problem.

Non-uniqueness of the travelling wave solutions in this model is discussed in [4–7]. In [5] the analysis based on the AEA is carried out for both solid and gaseous fuel for the cases of the zero and first-order reactions. It is clearly demonstrated that there can exist three solutions travelling with different veloc-

ities and burning temperatures. Also in [5] a brief report is given on the results of the numerical analysis of the model, which was done by the authors earlier. However to the best of our knowledge it has not appeared as a regular publication. In particular it is stated that the propagation regime corresponding to the intermediate flame speed is always unstable, whereas the branches with fast and slow flame speeds can be stable or lose stability in an oscillatory manner. In [6] the model is generalized to include an additional step $B \to C$ so that the resulting scheme is a combination of the two-step sequential and competitive reaction mechanisms. It is argued that the resulting model can be applied to the description of combustion of coal and mixtures of transition metals with boron. Further, the properties of the travelling combustion waves are studied and it was shown that regimes of flame propagation multiplicity are also possible. In [7] various two-step reaction models for combustion wave propagation are considered and in particular the model with parallel competing schemes is investigated. The simple mechanistic explanation based on the notion of the crossover temperature and the balance between the rates of the reactions and heat release is presented, which allows one to qualitatively describe the existence of two different types of the response curves: monotonic with the single travelling wave solution and 'S' -shaped with either one or three solutions. The AEA analysis is also carried out in [7]. In the most interesting case when the rates of both reactions are comparable the authors expand the solution near the crossover temperature and obtain the leading order equations for the temperature and fuel concentration in the reaction zone. However, the resulting inner problem has not been solved either analytically or numerically and the authors were not able to give any estimates for flame speed and temperature. In the case when one reaction is dominating, the problem is reduced to the usual one-step approximation which is similar to the conclusions in [3–6, 8].

The linear stability analysis of the travelling combustion wave in the model with two parallel competing reactions is carried out in [9]. Considering only zero-order reactions with an infinitely thin reaction zone (delta-function sources are the simplification adopted in [9]) allows the dispersion relation to be obtained

explicitly. The intermediate branch is again found to be unstable, whereas the fast and slow solution branches are either stable or exhibit pulsating instabilities, which agrees with the results communicated in [5].

In our earlier papers [10, 11] we have studied a similar problem of flame propagation in a model with competitive exo-endothermic reactions. Both properties and flame stability have been investigated numerically and analytically by means of AEA. However, the behaviour of combustion waves in this model is significantly different since the second reaction works as a chemical buffer absorbing the heat produced in the course of the first exothermic reaction. The result is that the endo-exothermic model exhibits behaviour more like the one-step non-adiabatic model.

The aim of the current paper is to undertake both linear and nonlinear stability analysis for the model of flame propagation with two-stage competing parallel reactions of the first-order. Our attention is mainly focused on the parametric region where the multiple solutions exist. Since under these conditions the interesting dynamical behaviour can occur. The paper is organized as follows. In section 2 the governing model equations are introduced and the methods used for the investigation are described. Section 3 focuses on the travelling wave solutions to the model detailed in section 2 where regions of multiplicity may exist in the parameter space. Section 4 presents the actual results of search for travel wave solutions and multiplicity while section 5 details the solutions stability and bistability. The article concludes with a brief discussion of the results.

2. Model and methods

We consider a diffusional-thermal model with two-step kinetics for premixed combustion wave propagation in one spatial dimension under adiabatic conditions. It is assumed that the reactant undergoes two competitive exothermic reactions: (R1) $A \to B$ and (R2) $A \to C$ with Arrhenius kinetics. The nondimensional equations governing this process can be found in [10] and are the

following

$$\begin{aligned} \frac{\partial u}{\partial t} &= \frac{\partial^2 u}{\partial x^2} + v\left(e^{-1/u} + q\,r\,e^{-f/u}\right), \\ \frac{\partial v}{\partial t} &= \frac{1}{L}\frac{\partial^2 v}{\partial x^2} - v\,\beta\left(e^{-1/u} + r\,e^{-f/u}\right), \end{aligned} \tag{1}$$

where t and x are non-dimensional time and space coordinates; u and v are the dimensionless temperature and fuel concentration; β is the dimensionless activation energy of the first exothermic reaction (R1); q is the ratio of the enthalpies, r is the ratio of pre-exponential factors, and f is the ratio of the activation energies of the second (R2) to the first (R1) exothermic reaction respectively; L is the Lewis number for the fuel. Here q is positive in contrast to [10, 11], where the second reaction is endothermic and thus q was negative.

Equations (1) are considered subject to the boundary conditions

$$\begin{aligned} &u = 0, \qquad v = 1, \qquad \text{for} \qquad x \to \infty, \\ &u_x = 0, \qquad v_x = 0, \qquad \text{for} \qquad x \to -\infty. \end{aligned} \tag{2}$$

On the right boundary we have a cold ($u = 0$) and unburned state ($v = 1$). The nondimensionalized ambient temperature is taken to be equal to zero. The assumption of zero ambient temperature is assumed here to circumvent the cold boundary problem, which has been discussed by many authors (e.g. see the discussion in [12]). On the left boundary ($x \to -\infty$) neither the temperature of the mixture nor the concentration of fuel can be specified. We only require that there is no reaction occurring so the solution reaches a steady state of (1). Therefore the derivatives of u and v are set to zero for $x \to -\infty$.

In this work we consider travelling wave solutions to (1). We make the substitution $\xi = x - c\,t$, where c is the constant speed of the travelling wave, into (1) and produce the system of ordinary differential equations

$$\begin{aligned} u_{\xi\xi} + c\,u_\xi + v\left(e^{-1/u} + q\,r\,e^{-f/u}\right) &= 0, \\ L^{-1}\,v_{\xi\xi} + c\,u_\xi - v\,\beta\left(e^{-1/u} + r\,e^{-f/u}\right) &= 0. \end{aligned} \tag{3}$$

The system (3) consists of two second-order ordinary differential equation and in this sense is similar to one-step models [12]. However, in contrast to one-step

models, here there is no additional integral, which can be used to reduce the order of the system (3) or to determine the downstream flame temperature as it is done in [12]. Therefore the burning temperature, $u_b = \lim_{x\to\infty} u(x,\ t)$ is undefined and should be considered as an eigenvalue of the problem as well as the flame speed.

The system of ordinary differential equations (3) together with boundary conditions (2) constitute the two-point boundary value problem, which is solved numerically by using a standard shooting algorithm with a fourth-order Runge-Kutta integration scheme first and then the results are corrected by employing the relaxation algorithm. Here the moving frame coordinate ξ is discretized using finite differences. As the domain required by the travelling fronts varies greatly from one parameter set to the next ξ is scaled to unity using an unknown parameter δ. After providing an initial guess for the solution profile the resulting nonlinear algebraic equations are solved iteratively using the Newton-Kantorovich method until the change from one iteration to the next is less than 10^{-15}. In addition to solving for u and v, equations for the scaling parameter δ and the front speed c are added to the system and solved.

The stability of the combustion waves is investigated in a way similar to [13]. We linearize the governing Eqs. (1) near the travelling wave solution. We seek solutions of the form $u(x,t) = U(\xi) + \epsilon\phi(\xi)e^{\lambda t}$, $v(x,t) = V(\xi) + \epsilon\psi(\xi)e^{\lambda t}$, where $[U(\xi),\ V(\xi)]$ represent the travelling combustion wave i.e. a solution to the problem (2, 3). Here terms proportional to the small parameter ϵ are the linear perturbation terms, λ is a spectral parameter governing the time evolution of the perturbation. Substituting this expansion into Eq. (1), leaving terms proportional to the first order of ϵ only, and introducing the vector function with components $\mathbf{v}(\xi) = [\phi,\ \psi,\ \phi_\xi,\ \psi_\xi]^T$ we obtain

$$\mathbf{v}_\xi = \hat{A}(\xi, \lambda)\mathbf{v}, \tag{4}$$

where

$$\hat{A} = \begin{bmatrix} 0 & \hat{I} \\ \hat{H} + \lambda\hat{Q} & -c\hat{Q} \end{bmatrix}, \quad \hat{Q} = \begin{bmatrix} 1 & 0 \\ 0 & L \end{bmatrix}, \tag{5}$$

Here $H(\xi)$ is a Wronskian of source terms in Eqs. (1) calculated at $U(\xi)$, $V(\xi)$ and $\hat{I}$ is 2×2 identity matrix. We will call a set, Σ, of all λ values for which there exists a solution to Eq. (4) bounded for both $\xi \to \pm\infty$ a spectrum of linear perturbations. In the general case, Σ is a set on the complex plane and it consists of the essential and the discrete spectrum. If there exists at least one $\lambda \in \Sigma$ such that $\mathrm{Re}\lambda > 0$, then the travelling wave solution is linearly unstable, otherwise, if for all $\lambda \in \Sigma$ the real parts are not positive, then the travelling wave solution is linearly stable. Therefore in order to investigate linear stability of the travelling wave solutions to Eq. (1), the spectrum Σ of the problem (4) has to be found. It can be shown (see [14] for details) that the essential spectrum consists of parabolic curves in the complex plane with $\mathrm{Re}\lambda \leq 0$. This implies that it is the discrete spectrum of the problem (4) that is responsible for the emergence of instabilities. The linear stability problem is solved by finding the location of the discrete spectrum on the complex plane using the Evans function method [15] as described in [13].

The nonlinear stability analysis as well as properties of the solutions bifurcating from the travelling waves are performed by direct integration of Eqs. (1). In order to simulate Eqs. (1) we employ the so-called method of lines [16]. The spatial dimension is discretised using the standard second-order center finite difference scheme. The resulting system of ordinary differential equations are stiff. The stiffness index of the discretized system behaves like $\sim 2/(\Delta x)^2$ where Δx is the distance between spatial points. Thus increasing the resolution of the spatial dimension greatly increases the stiffness of the system to be integrated. Further, the associated Jacobian of the system is sparse. Therefore we utilised the specialised stiff-solver for sparse problems MEBDFSO detailed in [17]. In all simulations presented here the relative and absolute tolerance was fixed to 10^{-6} and controlled by the MEBDFSO.

3. Travelling waves

In this section we focus on the investigation of the travelling wave solutions, which are found by numerically solving Eqns. (3) subject to boundary conditions (2) as described in previous section. Firstly, we discuss the conditions for the existence of multiple solutions. Following [7] the crossover temperature is introduced as a temperature, u^*, at which the rates of the second and first reactions are equal. By means of simple algebraic manipulations with the second equation in (3), it can be shown that $u^* = (f-1)/\ln r$. This definition has physical significance to the present competitive reaction scheme only if u^* is positive. Otherwise, if u^* is negative, one of the reactions is always dominating, the model behaves effectively as a one-step reaction model and no multiplicity occurs. For $u^* > 0$ there are two parameter regions: $\{f > 1,\, r > 1\}$ or $\{f < 1,\, r < 1\}$, which can be mapped to each other by the change of notation of the first and second reaction. Hence, in what follows we restrict the consideration to the case of $\{f > 1,\, r > 1\}$.

If the flame temperature is substantially below the crossover temperature then the first reaction is dominating and the flame speed and burning temperature is mainly defined by (R1). Thus the reaction terms proportional to r can be omitted in Eqns. (3) and we derive a standard one step model [12, 13] for which the flame speed and temperature can be written by using the AEA as

$$u_b^{(1)} = \beta^{-1}, \qquad c^{(1)} = \sqrt{2L\beta^{-1}}e^{-\beta/2}. \tag{6}$$

Similarly, if the flame temperature is much higher than u^* then (R2) is dominating and the flame speed and burning temperature is mainly defined by the second reaction step. In this case the first reaction terms in Eqns. (3) can be neglected and we once again derive the one step model, which after introducing new coordinate, $\xi' = \xi\sqrt{rq/f}$, time, $t' = trq/f$ and activation energy, $\beta' = \beta f/q$, can be written exactly in the same form as in [12, 13]. Thus once again we can use AEA formula (6) and obtain the flame speed and

temperature, which in the original variables can be expressed as

$$u_b^{(2)} = q\beta^{-1}, \qquad c^{(2)} = \sqrt{2Lrq^2\beta^{-1}f^{-2}}e^{-\beta f/2q}. \tag{7}$$

Comparing the equations for the flame speed (6, 7) and definition of the crossover temperature we see that there are two conditions for the activation energies, $\beta^{(1)} = \ln r/(f-1)$ and $\beta^{(2)} = q\ln r/(f-1)$, when the crossover temperature is equal to the burning temperatures for the one-step models governed by reactions (R1) and (R2), respectively. It is seen that depending on the value of q the temperatures, $u_b^{(1,2)}$, and activation energies, $\beta^{(1,2)}$, can be ordered in different ways.

If $q < 1$, then $u_b^{(2)} < u_b^{(1)}$ and $\beta^{(2)} < \beta^{(1)}$. In this case as we increase β from the values when $u^{(2)} \gg u^*$ (or $\beta \ll \beta^{(1)}$) the reaction (R2) is dominating and the flame temperature follows the dependence in Eqn. (7). As β approaches $\beta^{(2)}$ the reaction (R1) becomes important. The flame temperature switches from the colder branch corresponding to (R2) to the hotter branch corresponding to (R1) as β is increased from $\beta^{(2)}$ to $\beta^{(1)}$ in such a way that u_b is staying close to u^*. For the values of the activation energy higher then $\beta^{(1)}$, the dependence $u_b(\beta)$ approaches the limiting behaviour (6) corresponding to (R1). In other words, in the case when $q < 1$ there is no multiplicity and the flame temperature is monotonic function of activation energy with a characteristic plateau behaviour in the region $\beta^{(2)} < \beta < \beta^{(1)}$ when both reactions are significant. This situation is also discussed in [7].

In the case $q > 1$ the burning temperature, $u^{(2)}$, associated with (R2) is higher than $u^{(1)}$ and activation energies are also ordered differently, $\beta^{(1)} < \beta^{(2)}$. This situation is depicted in Fig. 1 for $L = 1$, $f = 1.5$, $q = 5$ and $r = 25$. The dependencies $u^{(1,2)}(\beta)$ are plotted with the dashed lines, where index '1' corresponds to the curve marked as '1 step slow branch' and index '2' to the curve labelled '1 step fast branch' respectively. The dot-dashed line corresponds to the crossover temperature, u^*, which crosses the curve $u^{(1)}(\beta)$ at $\beta^{(1)} \approx 6.3$, while the intersection with $u^{(2)}$ is for $\beta^{(2)} \approx 32$ and is not shown in the figure. Numerical calculations of the temperature, u, for parameter values $L = 1$,

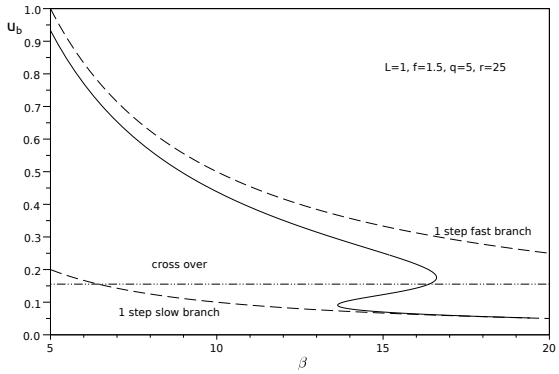

Figure 1: The burn temperature, u_b, against β for $L = 1$, $f = 1.5$, $q = 5$ and $r = 25$. The two dashed lines indicate the variation of the burn temperature for one-step reactions equivalent to the fast and slow branches. The dot-dashed line labelled "crossover" indicates the crossover temperature for this parameter set. Multiplicity of burning temperatures occurs in near the crossover temperature.

$f = 1.5$, $q = 5$, and $r = 25$ are also plotted in Fig. 1 with the solid line. It is seen that as the activation energy is increased from the values below both $\beta^{(1,2)}$ and the mixture is becoming less exothermic the flame temperature follows the formulae (7) for the one-step model governed by (R2). As the temperature decreases and approaches u^* the first reaction comes into play and the solution cannot follow the behaviour given by Eqns. (7). This causes the appearance of the first turning point close to the crossover temperature. Further decrease of the burning temperature causes the solution to turn backward and to approach the slower and colder branch governed by reaction (R1), which results in folding and occurrence of the intermediate lag of the $u(\beta)$ dependence. As u_b gets colder the second reaction freezes and the combustion wave is controlled by the reaction (R1). This causes the second turning point after which the solution rapidly approaches the limiting behavior defined by Eqns. (6).

Thus we see that the condition $q > 1$ is necessary for the onset of multiplicity. However, this condition is not sufficient as it is demonstrated in the Fig. 2, where the location of the turning points is plotted in the β vs. r plane for

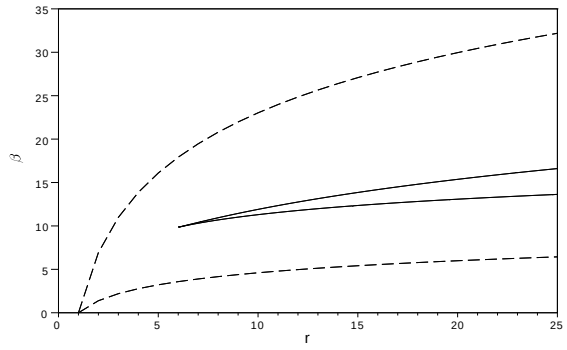

Figure 2: Dependence of the activation energies at the turning points on recombination parameter, r, for $L = 1$, $f = 1.5$, $q = 5$. The dashed curves show for what values of r and β the one-step burn temperature is equal to the crossover temperature i.e. $u_b = u^*$. The higher and the lower dashed curves are for the fast and slow branch equivalent one-step models, respectively. The solid line shows when $u_b = u^*$ in the full model (3). A multiplicity of burning temperatures exist for $r \geq 6$ for the case illustrated.

$L = 1$, $f = 1.5$, $q = 5$. The solid lines correspond to numerical solutions, whereas the dashed lines represent $\beta^{(1,2)}$. The region of multiple solutions is located between the curves.

As seen in Fig. 2 the simple analytic approximation of the conditions for emergence of multiplicity substantially overestimates the region where triple solutions exist, however qualitatively correctly predicts the location of the turning points.

4. Results

The insight gained from the crossover temperature concept does away with the need to search a 5-dimensional parameter space for regions of multiplicity. Provided f and q to be greater than unity we then only need to find the value of r for which multiplicity exists. This is illustrated in Fig. 3. For a fixed value of r the system (3) is solved for different β using the numerical methods mentioned earlier. For low activation energies the flame front speed tends asymptotically

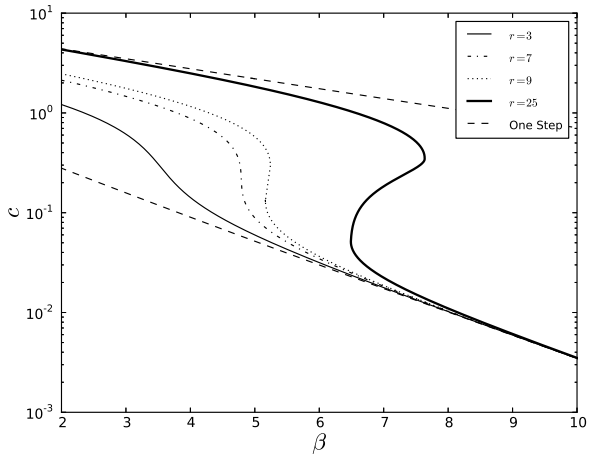

Figure 3: The onset of multiplicity as the parameter r is changed while $L = 2$, $q = 5$ and $f = 2$. The dashed lines show the behaviour of equivalent one-step models for the fast and slow branches. As r is increased the flame front speeds change from a monotonic curve to two discontinuous curves which exhibit multiplicity.

to the values predicted by (7) indicted by the upper dashed line in the figure. Likewise, for high activation energies, the flame front speeds are well described by (6) indicated by the lower dashed line. For $r = 3$ (thin solid line) and $r = 7$ (dot-dash line) the curve is monotonic and therefore is only one travelling wave solution for these parameters. At $r = 9$ the curve (dotted) is 'S'-shaped and there are in fact three solutions of system (3) for a thin range of β: the fast, slow and intermediate solutions. The crossover temperature analysis indicates that increasing r expands the range of β for which multiplicity exists. The remaining curve, for $r = 25$, in Fig. 3 confirms this analysis and the width of the multiplicity region is approximately unity.

Increasing f (requiring more energy to ignite R2 relative to R1) has the effect of increasing the crossover temperature. This in turn means that any multiplicity regions will appear at smaller values of β as the fast branch reaction will extinguish earlier. Larger f will also have the effect of compressing the width of the multiplicity region. The crossover temperature does not depend on L so

theoretically multiplicity should exist for competing parallel reactions regardless of whether gases or solids are involved. The weak dependence of the location of the turning points on the Lewis number is also shown latter in this paper in Figs. 5 and 7.

Although it is not shown here for brevity, the effect of variation of q on the existence of multiplicity was also investigated. It follows from Eqns. (6) and (7) that decreasing q makes the width of the region of multiplicity smaller in terms of β and at certain threshold value the turning points coalesce implying the disappearance of the multiplicity. These results were also confirmed by means of numerical calculations.

In Fig. 4 typical examples of flame front profiles are presented. The general shape of travelling waves in this model does not change greatly from one parameter set to another. What does change, by orders of magnitude, is the width of the reaction zone and the wave front speed. Figure 4 presents solutions from a region of multiplicity with parameters $L = 2$, $q = 5$, $r = 25$, $f = 1.6$ and $\beta = 12$. The upper plot is a profile from the slow branch with a speed $c \approx 0.0018$ and the scaling parameter, $\delta \approx 4000$. In contrast the lower plot has a profile from the fast branch and the values of c and δ differ from the slow branch by 2 orders of magnitude: $\delta \approx 25$ and $c \approx 0.46$.

5. Stability analysis

In this section we present the results of our investigation of flame stability. Having found where in the parameter space the multiple solution branches exist, its important to know the stability of solutions within the region. Linear stability analysis of the travelling wave solutions of system (3) was conducted via the Evans function method. Its feasible to consider a large range of parameters with high resolution as only ODEs are involved. Full nonlinear stability analyses was then conducted for a few select parameter values and comparisons between the two stability approaches were made.

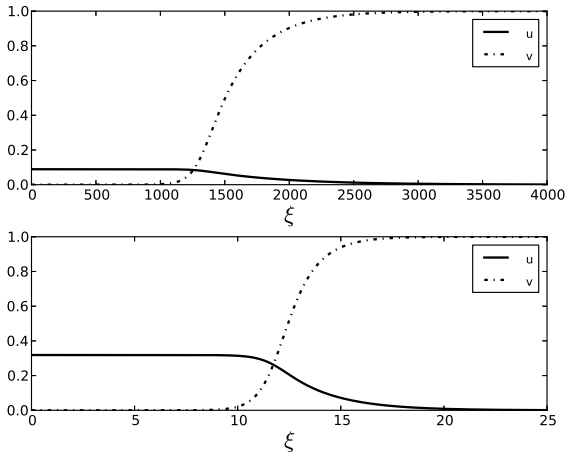

Figure 4: The travelling wave solutions with $L = 2$, $q = 5$, $r = 25$, $f = 1.6$ and $\beta = 12$ for the slow (upper axis) and fast (lower axis) branches. The speed of the slow flame front is $c = 0.0018359$ while the fast solution is $c = 0.46048$.

5.1. Linear stability

First we consider the stability of the fast branch for parameter sets exhibiting multiplicity. The stability analysis indicates that the flame front is stable for small and moderate values of β. As β is increased closer to the turning point the solution may lose stability. However, to investigate whether stability is lost before the turning point we consider the existence of Andronov-Hopf (AH) bifurcations. Using the Evans function the eigenvalues of the associated linear stability problem for given parameter can be found. Combining the Evans function and the standard Newton-Raphson method the condition for an AH bifurcation, $\mathrm{Re}\left[\lambda\left(\beta\right)\right] = 0$, can be solved for β. The existence of a AH bifurcation at some $\beta = \beta_{AH}$ means that the flame fronts have an oscillatory instability for $\beta \geq \beta_{AH}$.

Two possible scenarios for the fast branch are illustrated in Fig. 5. For all the curves presented $r = 25$ and $q = 5$. For three values of f the position of the AH bifurcation is drawn for a given value of β and L and is indicated by the solid lines. The dotted lines to which the solid lines approach represent

the position of the fast branch turning point for the respective value of f. We note here that L has only a weak influence on β_{TP}. For $L = 2$ and $f = 1.5$ no AH point exists. This means that the fast branch is stable right up until the turning point at β_{TP}. If, however, the Lewis number is increased to say, $L = 10$, then a AH point exists at $\beta_{AH} = 15.7$ and all flame fronts from the AH points until $\beta_{TP} = 16.8$ will have an oscillatory instability. The switching between the two scenarios occurs at the point where the AH and the turning point curves intersect. The point from which the AH locus originates and the fast solution branch changes from the completely stable to partly oscillatory unstable behaviour is a point of the Bogdanov-Takens bifurcation. For $f = 1.5$ it is located at $L = 2.265$.

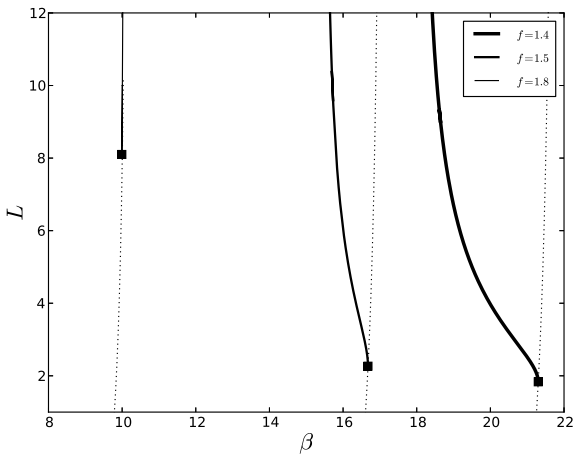

Figure 5: The position of the AH bifurcation and the turning points shown with the solid and dotted lines respectively for flame fronts from the upper branch with $r = 25$ and $q = 5$. For $f = 1.8$ (thinnest line) the difference between the AH curve and the turning point curve is small such that at the scale used in the figure there is no visible difference in the curves. The black squares indicate the position of the Bogdanov–Takens bifurcation.

The value of f has a strong influence on width of the range (β_{AH}, β_{TP}). Larger values of f drive the AH locus towards the turning point. For $f = 1.8$ and $L > 8$ the AH and the turning point locus are virtually identical. Further,

increasing f has the effect of lifting the value of L for which the AH curve begins i.e. the Bogdanov-Takens bifurcation point. Thus we see the fast branch is stabilised completely for mixtures with low Lewis numbers if f is large enough.

The spectra of the associated linear stability problem for $f = 1.5$, $L = 3$ and 10 are shown against the flame front speed in Fig. 6. The values of $Re\lambda$ are scaled over the flame speed in order to accommodate the range of eigenvalues variation on the same graph for flame speed changing two orders of magnitude. The spectrum is plotted against c so as to distinguish the fast to the mid branches. Starting from $c = 1$ and moving leftwards to lower speeds there is no curve drawn as $\mathrm{Re}(\lambda) \leq 0$ for the fast branch indicating linear stability. A AH bifurcation (■) occurs at $c \approx 0.3$. The real part of the spectrum becomes positive beyond the AH bifurcation and the eigenvalue is complex (dashed line) until the imaginary parts of the eigenvalues collide with each other and induce two, positive, purely real eigenvalues (solid lines). One real eigenvalue tends to zero as solutions approach the turning point (⧫), at $c \approx 0.1$, where the fast branch ends and the middle branch begins. The remainder of the curve for $L = 10$ is purely real and positive indicating the entirety of the middle branch is unstable. For $L = 3$ there is no AH bifurcation so the flame front is linearly stable for the entirety of the fast branch and stability is lost once the middle branch begins immediately after the turning point ($c \approx 0.07$).

A similar analysis was performed for the lower branch and the results are presented in Fig. 7. In addition to the AH loci (thick solid and dashed lines) and the slow branch turning point curves (vertical light dotted lines) there is a thick dotted line indicating the existence of AH bifurcations in the one-step model. The latter curve was obtained for the model which contains just the reaction R1. The slow solution branch is located to the right from the turning point curves. The stable solutions correspond to the parameter values below the AH curves. For given f if β is decreased up to the certain critical value the AH locus meets the turning point curve at the Bogdanov-Takens bifurcation point.

All stability curves considered here approach the one-step AH locus in the limit of large β, since in this limit the reaction R2 becomes frozen due to the

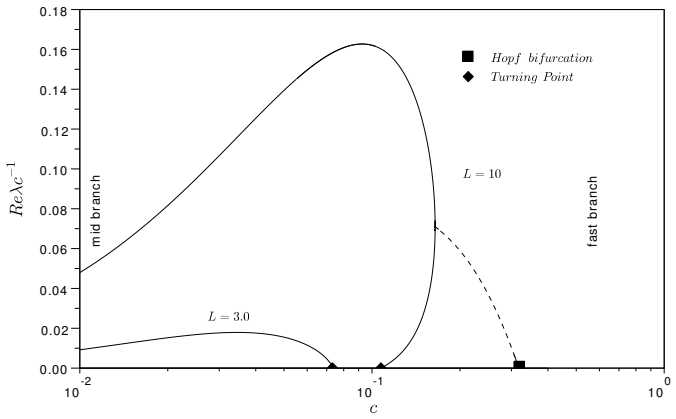

Figure 6: The positive real part of the spectrum against flame front speed for $r = 25$, $q = 5$ and two values of Lewis number: $L = 3$ and $L = 10$.

difference in activation energies. Increasing f has similar effect, thus for $f \geq 2.5$ the AH curve is indistinguishable from the one-step one (since R2 is not activated).

If $f \geq 2.5$ the flame front is linearly stable for β values in the whole range between the turning point and AH locus. However, for lower f values (curves for $f \leq 2.1$ in Fig. 7), the AH curve folds over indicating that for a given f and L there can be several situations. If L is above the folding point of $L(\beta)$ curve for AH bifurcation for the slow solution is completely unstable right from the turning point. If L is between the maximum value of $L(\beta)$ curve and the Bogdanov-Takens point there can be two AH bifurcations. If L is less then the Bogdanov-Takens bifurcation point, the slow solution is stable in the range of β values between the turning point and AH curves.

Consider the curve for $f = 2.05$ (thick solid curve in Fig. 7), if $L = 8$ then no AH bifurcation exists and the entirety of the slow branch is unstable. However, if $4 < L < 7.5$ then flame fronts are first unstable for $\beta_{TP} \leq \beta \leq \beta_{AH1}$, regain linear stability for $\beta_{AH} \leq \beta \leq \beta_{AH2}$, and become unstable again if $\beta > \beta_{AH2}$. Here β_{AH1} and β_{AH2} are the first and second crossing of the AH curve with the line $L = const$. Finally, if L is low enough, which for the case of $f = 2.05$ is $L < 4$, then the AH point exists for large β and the slow branch is linearly

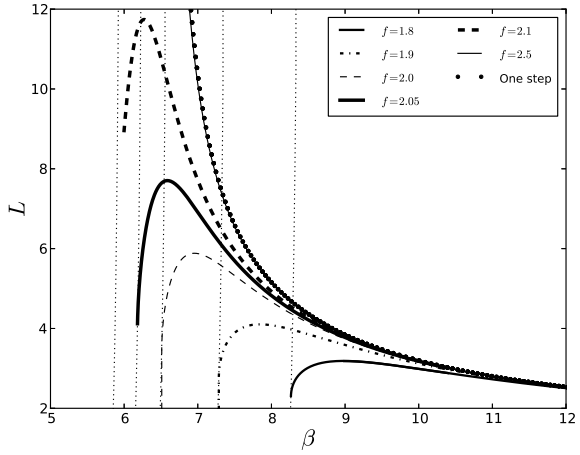

Figure 7: The position of the AH bifurcation and the turning points for flame fronts from the slow branch with $r = 25$ and $q = 5$. The position of the turning point for a given f is indicated by the vertical dotted line the associated AH curve approaches. For large β all AH curves approach the result for the one-step model.

stable in a wide range of β values. In these last two scenarios there exists the possibility of bistability.

The behaviour of the spectrum for the three scenarios of slow branch stability are presented in Fig. 8. Once again the eigenvalue is scaled over squared flame speed and plotted against c to show the mid and slow branches on the same graph. Three values of L are taken: $L = 1.5$, 3.0, 5.0. First consider the curve for $L = 1.5$ which is labelled '1' in the figure. At $c \approx 0.2$ we see the turning point (⧫) indicating the start of the middle branch. The eigenvalue is positive and purely real (solid curve) and reaches its maximum at $c \approx 0.06$ returning to zero at the second turning point denoting the beginning of the slow branch ($c \approx 0.02$). Thus the entirety of the middle branch of solutions is unstable as expected. For $c < 0.02$ there is no curve labelled '1' in the figure so the real value of λ is negative and the slow branch is linearly stable. Curve '2', for which $L = 3.0$, behaves in a similar fashion as curve '1' except once we approach the second turning point near the end of the middle branch. At $c \approx 0.025$ the middle

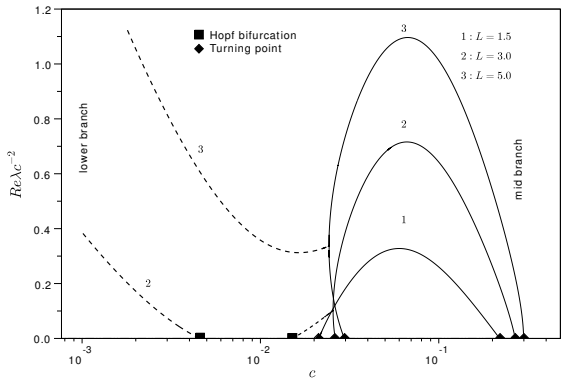

Figure 8: The positive real part of the spectrum against flame front speed for $r = 25$, $q = 5$, $f = 1.8$ and three values of Lewis number: $L = 1.5$, $L = 3$ and $L = 5$. Eigenvalues are only shown for middle and slow branch solutions. The middle branch is always unstable and the solid lines for all values of L indicates the eigenvalue is purely real.

branch ends and a second purely real eigenvalue emerges from the turning point. The two eigenvalues collide soon after the start of the slow branch and produce a complex eigenvalue (dashed line), the real part of which goes to zero at the AH bifurcation (■) near $c = 0.015$. There is now a region for which curve '2' is below the axis $Re\lambda = 0$ and here the flame fronts are linearly stable. A second AH point occurs at $c \approx 0.0045$ and slow flame fronts have an oscillatory instability. Lastly, curve '3' ($L = 5$) shows that the middle branch is unstable and once again a second real eigenvalue emerges from the turning point between the mid and slow branches. After the collision of the two real eigenvalues the real part of the resulting complex eigenvalue grows. Thus the slow branch is unstable too for $L = 5$.

The linear stability analysis provided by the Evans function technique predicts the fast branch is either completely stable or loses its stability close to the turning point through a oscillatory instability. How close it happens, strongly depends on the value of f. In cases of interest (i.e. moderate f values) the slow branch can be either completely stable, completely unstable, or has a region

between two AH bifurcations that is stable.

5.2. Pulsating solutions

To confirm the stability predicted in the previous section we performed a number of numerical simulations of system (1). In all cases a narrow Gaussian was used as the initial condition for the temperature profile to mimic an igniting spark or "hot spot". The fuel was initially set to unity for all x. During the simulation the flame front speed was continuously calculated as

$$c = \frac{\int_0^L \left|\frac{\partial v}{\partial t}\right| dx}{\int_0^L \|\nabla v\| \, dx}, \tag{8}$$

where L is the length of the numerical calculation domain and the simulation is continued until the speed has settled to a clear constant value.

Comparisons were made between the results obtained by solving the system (3) and associated stability problem and the integration of the full PDE model (1). Figure 9 shows the flame front speed determined from Eqs (3) where the solid line corresponds to stable and dashed line to unstable regimes according to the Evans function analysis. Only the fast branch is present and the turning point for the branch is at $\beta \approx 16.8$. The linear stability analysis predicts the fast branch to be stable until the AH bifurcation at $\beta \approx 15.7$. The solid dots give the flame front speed calculated during the simulations of the PDEs once transitory dynamics had dissipated. The PDE results are in good agreement with the ODE results up until the AH point. Pulsations in front speed are evident for simulations with β values beyond the AH bifurcation for which the instantaneous flame speed becomes a periodic function of time. In Fig. 9 this is indicated by the presence of two dots for a given value of β marking the local maximum and minimum of c. Period doubling of front speed occurs at $\beta = 16.2$. For greater values of β it was not clear what was happening and more simulations will be performed in the future work to ascertain the dynamics.

The flame front speed for $\beta = 16.2$ from Fig. 9 as a time series is detailed in Fig. 10. The speed cycles through 4 distinct extrema values which are

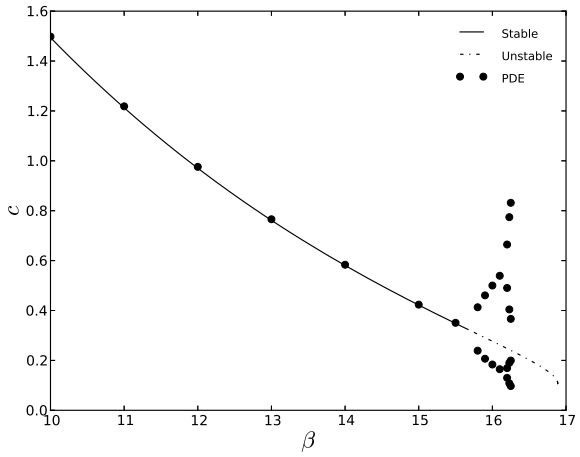

Figure 9: A comparison of the front speed, c, as calculated from the ODE system (3) and the full PDE model (1) for the fast branch of solutions with parameters $L = 10$, $f = 1.5$, $r = 25$ and $q = 5$. The solid and broken lines indicate stable and unstable travelling wave solutions respectively as determined by the Evans function analysis.

highlighted by the solid dots on the time series. The temperature profiles for exactly the times labelled with dots in Fig. 10 are shown in Fig. 11. Here the focus is only on the reaction zone. Instead of a smooth propagation of the front with a flat temperature profile behind the reaction zone the front proceeds in a "stuttering" fashion and the temperature profile has a peak near the reaction zone from which is decays and oscillates about some average temperature.

Similar simulations were performed for the slow branch with $L = 3$, $f = 1.8$, $r = 25$ and $q = 5$. Figure 12 details the comparison of results from ODE and PDE analysis. There are two AH bifurcations (■) which occur at $\beta = 8.48$ and $\beta = 9.96$. For β values between the AH bifurcations the flame front is propagating with a constant speed what is confirmed by simulations. The turning point for the fast branch is at $\beta = 9.88$ (dotted line) which is stable everywhere (see Fig. 5) so bistability exists for these parameter values. Pulsations in front speed are evident in simulations but decay slowly for stable fronts and grow in unstable fronts. Pulsations are most pronounced for β values close to the slow

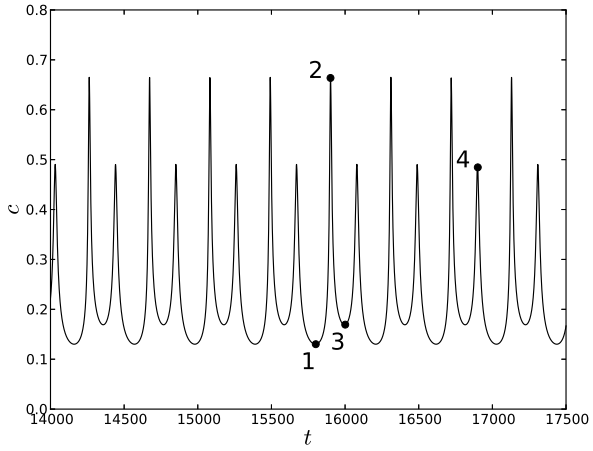

Figure 10: The speed for a front from the fast branch with parameters $L = 10$, $f = 1.5$, $r = 25$, $q = 5$ and $\beta = 16.2$. The value of c clearly cycles through 4 different values which are indicated in the figure by the numbers. This behaviour is period doubling of the speed and could indicate the onset of chaos for higher values of β.

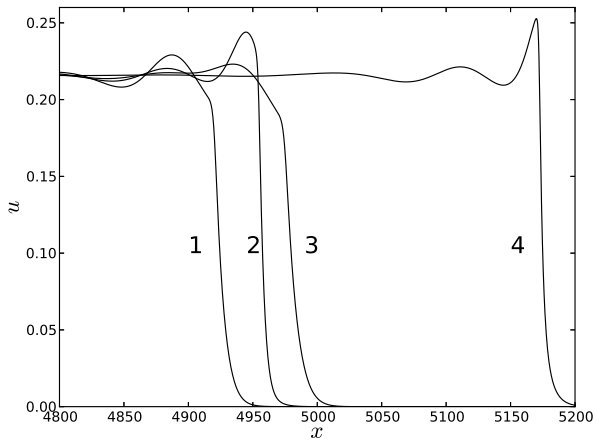

Figure 11: The temperature profiles for a front from the fast branch with parameters $L = 10$, $f = 1.5$, $r = 25$, $q = 5$ and $\beta = 16.2$. The profiles, labelled 1 to 4, are taken at times correspondingly labelled in figure 10.

branch turning point at $\beta \approx 8.25$.

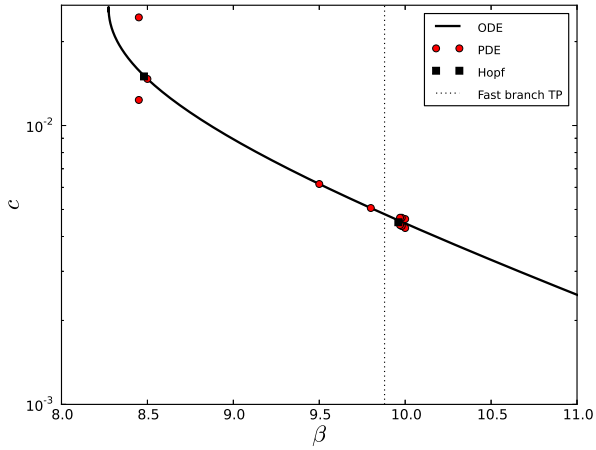

Figure 12: A comparison of the front speed, c, as calculated from the ODE system (3) and the full PDE model (1) for the slow branch of solutions with parameters $L = 3$, $f = 1.8$, $r = 25$ and $q = 5$.

5.3. Bistability and switching

The ODE analysis demonstrated the existence of not only multiplicity of flame front speeds in the model but also bistability. This was confirmed by simulation of the full PDE model. Bistability allows the possibility of switching rapidly between the fast and slow reactions and vice versa. Figure 13 demonstrates the concept. Starting at a flame front with a speed such that its near the first turning point (solid dot) the activation energy, β, is peturbed to a higher value of β. The fast reaction will now be extinguished leaving only a slow reaction flame front. The switching is indicated by the arrow in Fig. 13 and the final flame front speed is shown as the solid dot at the arrowhead. It may be possible to cause switching in a regime of combustion by a global change of the system such as a variation in pressure or "doping" of the combustive material so that its no longer homogeneous and the inhomogeneity is enough to perturb the flame front.

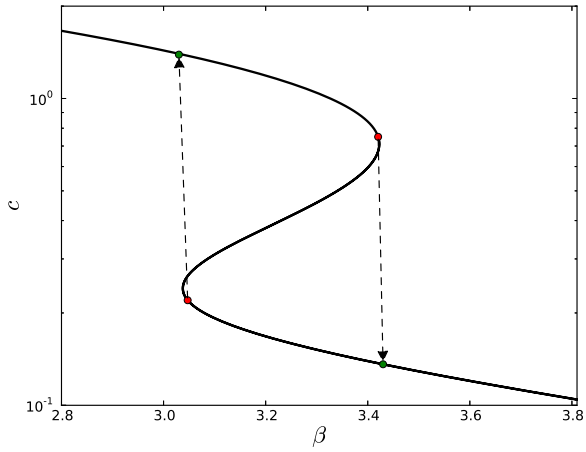

Figure 13: The speeds of flame fronts as found numerically from (3) with varying β and $L = 2$, $q = 5$, $r = 25$ and, $f = 3$. For values of β outside the domain of the figure the speed of the flame tends to the appropriate one-step model asymptotic value. The dots at the base of an arrow indicates the speed and the associated initial conditions used in PDE simulations where switching between the two stable branches of travelling wave solutions is induced. The speed and associated conditions after the switching are indicated by the dots at the head of an arrow.

We present two numerical simulations of system (1) which demonstrate that if such a perturbation could be made then the switching is stable in the sense that after the perturbation the flame front is able to settle to a constant speed. For the parameter values $L = 2$, $q = 5$, $r = 25$, $f = 3$ the temperature and fuel profiles were found for $\beta = 3.047$ (slow branch) and $\beta = 3.42$ (fast branch). Both solutions are linearly stable. These profiles were then used as the initial conditions in the simulations — the only exception made to our usual Gaussian initial condition. Using the exact profile as the initial condition to a simulation avoids the some times lengthy process of the Gaussian spike reforming to the flame front solution for the given parameters. The profiles are propagated for 1000 time units and the value of β was changed: from $\beta = 3.047$ to $\beta = 3.03$ in the case of the switch from slow to fast branches; and from $\beta = 3.42$ to $\beta = 3.43$ in the case of the switch from fast branch to slow. What can be seen in Figs.

14 and 15 is the propagation of the initial condition for $0 \leq t \leq 1000$ where the flame front speed is constant and agrees with the values calculated by ODE analysis in Fig. 13. At $t = 1000$ (vertical dashed lines in both figures) the value of β is changed and the flame front speeds go through a transitory phase of 500 to 1000 time units. The profiles have then fully reformed for the new conditions and the speeds reach constant values. The new speed values are significantly different to the initial speeds and match the values of the opposite branch as found by the ODE analysis.

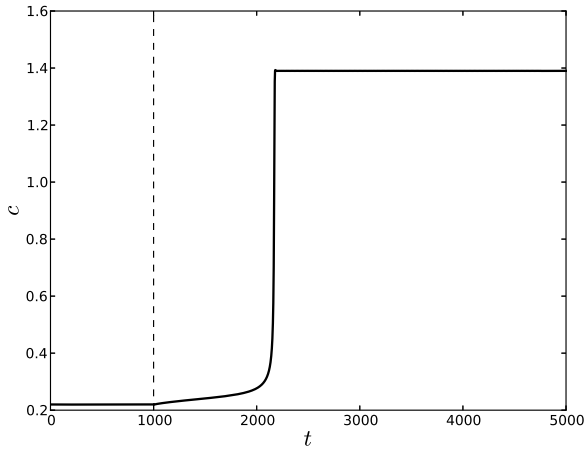

Figure 14: The flame front speed for the parameters $L = 2$, $q = 5$, $r = 25$, $f = 3$ and initially $\beta = 3.047$. At $t = 1000$ the parameter $\beta = 3.03$ and the flame front goes through a transitory phase which ends at $t \approx 2000$. The speed increases from $c = 0.22$ to $c = 1.39$ and the transition from the slow branch solution to the fast solution, as illustrated in Fig. 13, is complete.

6. Conclusion and discussion

In this paper we numerically investigated a diffusional-thermal model with two-step competitive exothermic reactions for premixed combustion wave propagation in one spatial dimension under adiabatic conditions. The analysis was done by using the shooting-relaxation, Evans function and direct PDE integration methods. We studied the conditions for multiplicity of the travelling

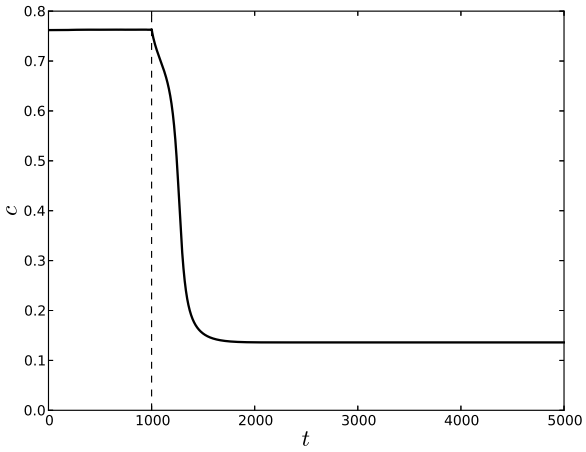

Figure 15: The flame front speed for the parameters $L = 2$, $q = 5$, $r = 25$, $f = 3$ and initially $\beta = 3.42$. At $t = 1000$ the parameter $\beta = 3.43$ and the flame front goes through a transitory phase which ends at $t \approx 1500$. The speed decreases from $c = 0.75$ to $c = 0.136$ and the transition from the fast branch solution to the slow branch solution, as illustrated in Fig. 13, is complete.

combustion waves and examined the stability of the solutions under the conditions of multiplicity.

A simple mechanistic explanation of the multiplicity phenomena was given based on the notion of the crossover temperature in the spirit of the analysis in [7]. This allows to qualitatively predict the regions in the parameter space where triple travelling combustion waves exist, which are then investigated numerically. The numerical analysis confirms that for certain parameter values the dependence of the flame on activation energy is triple-valued 'S'-shaped function i.e. for given external conditions there are three solutions travelling with different velocities: fast, mid and slow solutions, which are separated by two turning point (or fold) bifurcations. The width of the multiplicity region in the parameter space is investigated and conditions are found for which the turning points merge and the triple solution is replaced with a single one.

The linear stability analysis was carried out and it was shown that the fast

solution is either completely stable up to the turning point or exhibit oscillatory instability due to the AH bifurcation prior to the turning point has been reached. In this case two complex conjugate points of the discrete spectrum of the linear stability problem move from the left half to the right half of the complex plane causing the emergence of oscillatory instabilities. The neutral stability boundary and the turning point loci were found in the space of parameters. It was demonstrated that the oscillatory instability originates from the Bogdanov-Takens bifurcation – a point in the space of parameters where the turning point and AH loci merge. The mid branch was found to be completely unstable from one turning point to the other, which is characterised by the existence of purely real eigenvalue in the right half of the complex plane. As for the slow solution branch the situation is more complex. The analysis of the location of the turning point and AH loci in the parameter space indicates that there are three scenarios resulting in the loss of stability as the activation energy is increased for other parameters being fixed: (i) The slow branch can be completely unstable from the turning point condition. (ii) There can be a single AH bifurcation so that the slow branch is stable for the range of activation energies between the turning point and the AH bifurcation conditions, and loses stability in the oscillatory manner for activation energies higher then the critical values for the AH bifurcation. (iii) There are two AH bifurcations for the slow branch so that the solution is unstable from the turning point to the first AH bifurcation, stable for activation energies between the two AH bifurcations, and unstable again for the activation energies higher then the second AH bifurcation point. The critical conditions for the AH and turning point bifurcations was studied in the space of parameters and it was demonstrated that there exist conditions of bistability i.e. a situation when both the fast and slow solutions are stable.

The nonlinear stability analysis was also carried out. It is demonstrated that the AH bifurcations observed were supercritical. A stable limit cycle emerges as the neutral stability boundary is crossed. In terms of the original problem this implies that the stable pulsating solutions bifurcate from the travelling solution

branches due to the AH bifurcation. As the activation energy is varied away from the neutral stability boundary the amplitude of oscillations of the instantaneous flame speed increase and at certain stage the period doubling bifurcation occurs. It is not clear at the moment what kind of complex dynamical behaviour can be encountered as the bifurcation parameter is further increased. This is going to be the subject of our future work. It was also demonstrated that the dependence of the flame speed on the activation energy can show the hysteresis type of behaviour. In particular decreasing (or increasing) the activation energy below (or above) the turning point conditions may result in sudden very abrupt acceleration (or deceleration) of the flame velocity so that the speed can rapidly change in orders of magnitude in a very short time interval. Such issues may be of practical interest for example in fire safety and will be studied in our future work.

7. Acknowledgements

I. N. Towers acknowledges the hospitality and assistance of the P. N. Lebedev Physical Institute where much of this work was undertaken. V.V. Gubernov, A.V. Kolobov and A.A. Polezhaev acknowledge the financial support from the Russian Foundation for Basic Research grant 11-01-00392 and the Dynasty Foundation. H.S. Sidhu acknowledges the support of the Australian Research Council Grant DP0878146.

[1] N. A. Martirosyan, S. K. Dolukhanyan, A. G. Merzhanov, Combustion, Explosion and Shock Waves, 19 (1983) 711-712. [In Russian: Fizika Goreniya i Vzryva 19 (1983) 22-24.]

[2] N. A. Martirosyan, S. K. Dolukhanyan, A. G. Merzhanov, Combustion, Explosion and Shock Waves 19 (1983) 569-571. [In Russian: Fizika Goreniya i Vzryva 19 (1983) 39-42.]

[3] V. S. Berman, Iu. S. Riazantsev, Journal of Applied Mathematics and Mechanics 39 (1975) 286-296. [In Russian: PMM 39 (1975) 306-315.]

[4] I. S. Lyubchenko, D. M. Puchkov, and G.N. Marchenko, Combustion, Explosion and Shock Waves 18 (1982), 26-32. [In Russian: Fizika Goreniya i Vzryva 18 (1982) 34-42.]

[5] [In Russian] B. I. Khaikin, S. I. Khudyaev, "Nonuniqueness of stationary propagation of the combustion zone in the case of parallel reactions," Preprint, Chernogolovka (1978).

[6] E. A. Nekrasov, A. M. Timokhin, Combustion, Explosion and Shock Waves 22 (1986) 431-437. [In Russian: Fizika Goreniya i Vzryva 22 (1986) 48-55.]

[7] P. Clavin, P. Fife, I. Nicolaenko, SIAM J. Appl. Math., 47 (1987), 296-331.

[8] Ya. B. Zeldovich, G. I. Barenblatt, V. B. Librovich, G. M. Makhviladze, The mathematical theory of combustion and explosion, Consultants Bureau, New York, 1985.

[9] A. P. Aldushin, S. G. Kasrayan, [In Russian] Khim. Fiz., 10 (1982), 1412-1420.

[10] V. V. Gubernov, J. J. Sharples, H. S. Sidhu, A. C. McIntosh, J. Brindley, Journal of Mathematical Chemistry 50 (2012), 2130-2140.

[11] J. J. Sharples, H. S. Sidhu, A. C. McIntosh, J. Brindley, V. V. Gubernov, IMA J. Appl. Math., 77 (2012), 18-31.

[12] Weber, R. O., Mercer, G. N., Sidhu, H. S., Gray, B. F., Proc. R. Soc. London Ser. A, 453 (1997), 1105–1118.

[13] Mercer, G.N., Sidhu, H.S., Weber, R.O., Gubernov, V., SIAM Journal on Applied Mathematics, 63 (2003), 1259–1275.

[14] B. Sandstede, in: B. Fiedler (Ed.), Handbook of Dynamical Systems II, Elsevier, North-Holland, 2002, pp. 983–1055.

[15] J. W. Evans Indiana Univ. Math. J. 22 (1972) 577-593.

[16] A. V. Wouwer, P. Saucez, W. Schiesser, in: A. V. Wouwer, P. Saucez, W. E. Schiesser(Eds.), Adaptive Method of Lines, Chapman and Hall, Boca Raton, 2001.

[17] T. J. Abdulla, J. R. Cash, M. T. Diamantakis, Computers and Mathematics with Applications 42 (2001) 121-129.